

# Neutrinos help reconcile Planck measurements with both Early and Local Universe

Cora Dvorkin\*

*Institute for Advanced Study, School of Natural Sciences, Einstein Drive, Princeton, NJ 08540, USA*

Mark Wyman

*New York University, Center for Cosmology and Particle Physics, New York, NY 10003*

Douglas H. Rudd

*Kavli Institute for Cosmological Physics, Research Computing Center,  
University of Chicago, Chicago, Illinois 60637, U.S.A*

Wayne Hu

*Kavli Institute for Cosmological Physics, Department of Astronomy & Astrophysics,  
Enrico Fermi Institute, University of Chicago, Chicago, Illinois 60637, U.S.A*

In light of the recent BICEP2 B-mode polarization detection, which implies a large inflationary tensor-to-scalar ratio  $r_{0.05} = 0.2^{+0.07}_{-0.05}$ , we re-examine the evidence for an extra sterile massive neutrino, originally invoked to account for the tension between the cosmic microwave background (CMB) temperature power spectrum and local measurements of the expansion rate  $H_0$  and cosmological structure. With only the standard active neutrinos and power-law scalar spectra, this detection is in tension with the upper limit of  $r < 0.11$  (95% confidence) from the lack of a corresponding low multipole excess in the temperature anisotropy from gravitational waves. An extra sterile species with the same energy density as is needed to reconcile the CMB data with  $H_0$  measurements can also alleviate this new tension. By combining data from the Planck and ACT/SPT temperature spectra, WMAP9 polarization,  $H_0$ , baryon acoustic oscillation and local cluster abundance measurements with BICEP2 data, we find the joint evidence for a sterile massive neutrino increases to  $\Delta N_{\text{eff}} = 0.98 \pm 0.26$  for the effective number and  $m_s = 0.52 \pm 0.13$  eV for the effective mass or  $3.8\sigma$  and  $4\sigma$  evidence respectively. We caution the reader that these results correspond to a joint statistical evidence and, in addition, astrophysical systematic errors in the clusters and  $H_0$  measurements, and small-scale CMB data could weaken our conclusions.

The recent detection of degree scale B-mode polarization in the Cosmic Microwave Background (CMB) by the BICEP2 experiment [1] implies that the inflationary ratio of tensor-to-scalar fluctuations is  $r_{0.05} = 0.2^{+0.07}_{-0.05}$ , a number in significant tension with the upper limit of  $r < 0.11$  at 95% confidence level from the temperature anisotropy spectrum in the simplest inflationary  $\Lambda$ CDM cosmology [2]. This conflict occurs because the large angle temperature excess implied by the gravitational waves is not observed, and the mismatch cannot be compensated by parameter changes in this highly restricted, seven parameter model.

Aside from the possibility of large astrophysical [1, 3, 4] or cosmological [5–9] foreground and systematic contamination, possible solutions include extending the inflationary side or the  $\Lambda$ CDM side of this model. Inflationary modifications include a large running of the scalar tilt [1]; more explicit features in the inflationary scalar spectra [10–12]; or anticorrelated isocurvature perturbations [13]. In the present work, we instead consider extensions to the matter content of the  $\Lambda$ CDM model that can alleviate this early Universe tension.

In the  $\Lambda$ CDM cosmology, recall that the Planck CMB temperature anisotropy spectrum is also in conflict with

measurements of the local Universe [14–16]. The  $\Lambda$ CDM values for the current expansion rate – or Hubble constant,  $H_0$  – and the abundance of galaxy clusters are individually in  $2 - 3\sigma$  tension with direct measurements. While similar tensions existed in previous CMB data sets (e.g. [17]), the Planck results suggest a shift in the sound horizon that brings close agreement between CMB-based  $H_0$  inferences and baryon acoustic oscillation (BAO) measurements while disfavoring other possible explanations related to cosmic acceleration physics.

In this work, we show that both the early Universe and the local Universe tension with the Planck data may be pointing to the same extension of the  $\Lambda$ CDM cosmology: an extra massive sterile neutrino. Such a neutrino would modify the sound horizon at recombination, which is used to infer distances with both the CMB and BAO, removing the tension with local measurements of the Hubble constant. By changing the relationship between the CMB sound horizon and the damping scale, it also leads to an increase in the scalar tilt that suppresses large angle anisotropy relative to the simpler model. Finally, if the neutrino carries a mass in the eV range it suppresses the growth of structure and hence reduces the number of galaxy clusters predicted in the local Universe.

In §I we define the  $\Lambda$ CDM model along with its tensor and neutrino extensions and group the data sets by the early and local Universe tensions they expose. We

---

\* cdvorkin@ias.edu

present results in §II and discuss them in §III.

## I. MODELS AND DATA

The simplest inflationary  $\Lambda$ CDM model is characterized by 6 parameters,  $\{\Omega_c h^2, \Omega_b h^2, \tau, \theta_{\text{MC}}, A_s, n_s\}$ . Here,  $\Omega_c h^2$  represents the physical cold dark matter (CDM) density,  $\Omega_b h^2$  is the baryon density,  $\tau$  is the Thomson optical depth to reionization,  $\theta_{\text{MC}}$  is a proxy for the angular acoustic scale at recombination,  $A_s$  is the amplitude of the initial curvature power spectrum at  $k = 0.05 \text{ Mpc}^{-1}$ , and  $n_s$  its spectral index.

To these parameters we add  $r$ , the tensor-scalar ratio evaluated at  $k = 0.002 \text{ Mpc}^{-1}$ , and take the tensor tilt to follow the consistency relation  $n_t = -r/8$ . For the neutrino extension we add two new parameters. The first is the effective number of relativistic species,  $N_{\text{eff}}$ , defined in terms of the relativistic energy density at high redshift

$$\rho_r = \rho_\gamma + \rho_\nu = \left[ 1 + \frac{7}{8} \left( \frac{4}{11} \right)^{4/3} N_{\text{eff}} \right] \rho_\gamma. \quad (1)$$

In the minimal model,  $N_{\text{eff}} = 3.046$  and so  $\Delta N_{\text{eff}} = N_{\text{eff}} - 3.046 > 0$  indicates the presence of extra relativistic particle species in the early Universe. We assume that the active neutrinos have  $\sum m_\nu = 0.06 \text{ eV}$  (as suggested by a normal hierarchy and solar and atmospheric oscillation measurements [18]) and any additional contributions are carried by a mostly sterile state, with effective mass  $m_s$  for a total neutrino contribution to the energy density today of

$$(94.1 \text{ eV}) \Omega_\nu h^2 = (3.046/3)^{3/4} \sum m_\nu + m_s. \quad (2)$$

Thus  $m_s$  characterizes extra non-CDM energy density rather than the true (Lagrangian) mass of a neutrino-like particle. In particular even in the  $\Delta N_{\text{eff}} \rightarrow 0$  limit, at fixed  $m_s$ , the presence of an extra sterile species still adds an extra energy density component at recombination and still changes inferences based on the sound horizon.

In the most recent version of CosmoMC [19], a prior on the physical mass of a thermally produced sterile neutrino is imposed with a value of  $m_s/(\Delta N_{\text{eff}})^{3/4} < 10 \text{ eV}$  to close off a degeneracy between very massive neutrinos and cold dark matter.

We call these extensions the  $\nu\Lambda$ CDM and  $\nu r\Lambda$ CDM models, where the names follow from the additional parameters introduced by tensors and neutrinos.

For the data sets, we consider combinations that best expose the separate early and local Universe tensions with what we refer to as the central (C) Universe – the time intermediate between inflation at the late Universe, characterized chiefly by the CMB temperature power spectrum. This C data set is composed of the Planck temperature [2], WMAP9 polarization [20], and ACT/SPT [21–23] high multipole power spectra. For the Planck data analysis we marginalize over the standard

	Models
$\Lambda$ CDM	$\{\Omega_c h^2, \Omega_b h^2, \tau, \theta_{\text{MC}}, A_s, n_s\}$
$r\Lambda$ CDM	$\Lambda$ CDM + $r$
$\nu\Lambda$ CDM	$\Lambda$ CDM + $N_{\text{eff}} + m_s$
$\nu r\Lambda$ CDM	$\Lambda$ CDM + $N_{\text{eff}} + m_s + r$
	Data sets
C	{Planck, WP, SPT/ACT}
EC	C+BICEP2
CL	C + $H_0$ + BAO + Clusters
ECL	C+BICEP2 + $H_0$ + BAO + Clusters

TABLE I. Model and data set combinations. All models include  $\Lambda$ CDM parameters. All data sets include the central Universe (C) set.

Planck foreground parameters [2]. For the early Universe tension, we add to these what we call the early (E) data set, the BICEP2 BB and EE polarization band-powers [1]. We call the combination of these two the early-central (EC) Universe data set.

For the local Universe tension, we define the following collection as the local (L) data sets: the  $H_0$  inference from the maser-cepheid-supernovae distance ladder,  $h = 0.738 \pm 0.024$  [24], BAO measurements [25–27], and the X-ray derived cluster abundance using the likelihood code<sup>1</sup> of Ref. [29] which roughly equates to a constraint on  $S_8 = \sigma_8(\Omega_m/0.25)^{0.47} = 0.813 \pm 0.013$ . Note that the BAO data are added here not because they are in tension with Planck (they are not) but because they exclude resolutions of the  $H_0$  tension involving exotic dark energy or curvature. To these we again add the Planck temperature, WMAP9 polarization and the ACT/SPT data sets. We call this the central-local (CL) Universe data set. Finally, we call the union of this with the EC data the ECL data set. These model and data choices are summarized in Tab. I.

We analyze these data and models using the Markov Chain Monte Carlo technique and the CosmoMC code [19]. Our local analysis will be in many ways similar to that performed in Ref. [14] to which we refer the reader for details and robustness checks.

<sup>1</sup> This prescription employs the total matter power spectrum. More recent studies of the cluster abundance indicate that this may somewhat underestimate the neutrino mass at least at lower masses than considered here [28] where the abundance follows the cold dark matter power spectrum more closely. We continue to adopt this approach to be conservative with respect to new neutrino physics and provide a continuous limit with CDM at high  $m_s$ .

	$\nu r\Lambda\text{CDM-EC}$	$\nu\Lambda\text{CDM-CL}$	$\nu r\Lambda\text{CDM-ECL}$
$\Delta N_{\text{eff}}$	$1.06 \pm 0.37$	$0.62 \pm 0.28$	$0.98 \pm 0.26$
$m_s$ [eV]	$< 0.22$	$0.48 \pm 0.15$	$0.52 \pm 0.13$
$r$	$0.19 \pm 0.05$	–	$0.22 \pm 0.05$
$100\Omega_b h^2$	$2.268 \pm 0.043$	$2.267 \pm 0.028$	$2.276 \pm 0.027$
$\Omega_c h^2$	$0.132 \pm 0.005$	$0.122 \pm 0.005$	$0.127 \pm 0.004$
$100\theta_{\text{MC}}$	$1.040 \pm 0.001$	$1.041 \pm 0.001$	$1.040 \pm 0.001$
$\tau$	$0.100 \pm 0.015$	$0.096 \pm 0.014$	$0.097 \pm 0.014$
$\ln(10^{10} A_s)$	$3.136 \pm 0.033$	$3.107 \pm 0.031$	$3.117 \pm 0.030$
$n_s$	$0.999 \pm 0.017$	$0.985 \pm 0.012$	$1.001 \pm 0.010$
$h$	$0.74 \pm 0.04$	$0.70 \pm 0.01$	$0.72 \pm 0.01$
$S_8$	$0.89 \pm 0.03$	$0.81 \pm 0.01$	$0.81 \pm 0.01$

TABLE II. Parameter constraints (68% confidence level) with various model and data assumptions. Note that the  $\nu\Lambda\text{CDM-CL}$  case is in a different, no tensor model, context than the others which affects parameter interpretations.

## II. RESULTS

We begin by discussing the tension introduced by the BICEP2 data in the EC data set in the  $r\Lambda\text{CDM}$  model and its alleviation in the  $\nu r\Lambda\text{CDM}$  space independently of the CL data.

In Fig. 1, we show the posterior probability distribution of the scalar-tensor ratio in these two models. In order to compare distributions with the quoted BICEP2 result of  $r_{0.05} = 0.2^{+0.07}_{-0.05}$ , we show results for the ratio at  $k = 0.05 \text{ Mpc}^{-1}$  unlike the  $0.002 \text{ Mpc}^{-1}$  value assumed elsewhere. Note that in  $r\Lambda\text{CDM}$  the C data set imply an upper limit of  $r_{0.05} < 0.1$  consistent with the Planck collaboration analysis [2] but in tension with the E or BICEP2 data. Moving to the  $\nu r\Lambda\text{CDM}$  space, constraints on  $r_{0.05}$  weaken and allow  $r_{0.05} = 0.2$  within the 95% confidence limits.

In Fig. 2 we show the two dimensional  $r-\Delta N_{\text{eff}}$  posterior for the EC data and the  $\nu r\Lambda\text{CDM}$  model. Note in particular that  $r \sim 0.2$  would favor a fully populated  $\Delta N_{\text{eff}} \sim 1$  extra neutrino state, while  $\Delta N_{\text{eff}} = 0$  is significantly disfavored (at  $2.9\sigma$  once  $r$  is marginalized, see Tab. II). The origin of this preference is exposed by examining the  $n_s-\Delta N_{\text{eff}}$  plane in Fig. 3. Extra neutrino energy density at recombination allows a higher tilt and hence removes excess power in the low multipole temperature anisotropy. For example changing  $n_s$  from 0.96 to 1 reduces the amount of power at  $k = 0.002 \text{ Mpc}^{-1}$  relative to  $0.05 \text{ Mpc}^{-1}$  by 0.88, a reduction comparable to the amount of temperature power added by tensors when  $r = 0.2$ .

This change simultaneously relaxes the CMB- $\Lambda\text{CDM}$  upper bound on  $H_0$ , as can be seen in Fig. 4. Extra neutrino energy density at recombination changes the amount of time sound waves propagate in the CMB-baryon plasma and hence the standard ruler for CMB and BAO distance measures.

Note that the EC data set does not incorporate late Universe measurements of  $H_0$  or  $S_8$ . It is therefore interesting to compare the posterior probability of these

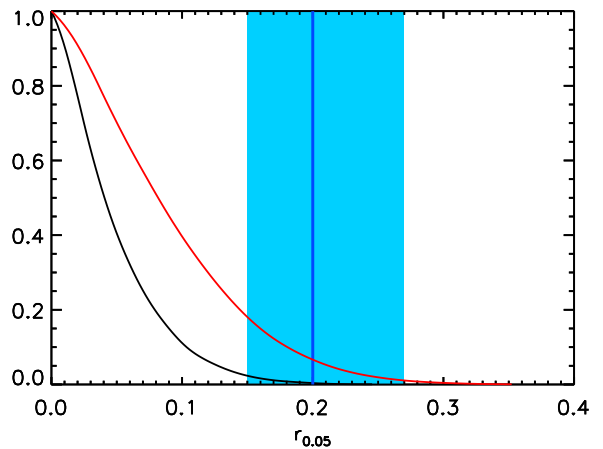


FIG. 1. BICEP2 measurement of the tensor-scalar ratio  $r_{0.05}$  (bands) compared with the posterior probability distribution of the C data set in the  $r\Lambda\text{CDM}$  model space (black curve) and  $\nu r\Lambda\text{CDM}$  space (red curve). In the former, the measurement is in strong tension with the posteriors whereas the addition of massive sterile neutrinos in the latter allows high  $r$ . For both the curves and the band, the tensor-to-scalar ratio is evaluated at a pivot scale of  $k = 0.05 \text{ Mpc}^{-1}$  unlike elsewhere.

parameters with the actual measurements before combining them into a joint likelihood. In Fig. 5, we show these distributions from the  $\nu r\Lambda\text{CDM-EC}$  analysis. Predictions for  $H_0$  in this model context are now fully compatible with measurements (bands) and correspond to  $0.74 \pm 0.04$ . The addition of tensors shifts the distribution to higher  $H_0$  as compared with neutrinos alone (cf. [14]). The predicted value of the cluster observable is  $S_8 = 0.89 \pm 0.03$ , so residual tension remains – albeit slightly less tension than with neutrinos alone. However, this posterior can accommodate the local observations within the 95% confidence range. This tension can be further reduced if there is a 9% upward shift in the mass calibration of clusters, which is currently allowed [29].

Likewise it is instructive to review the local tension

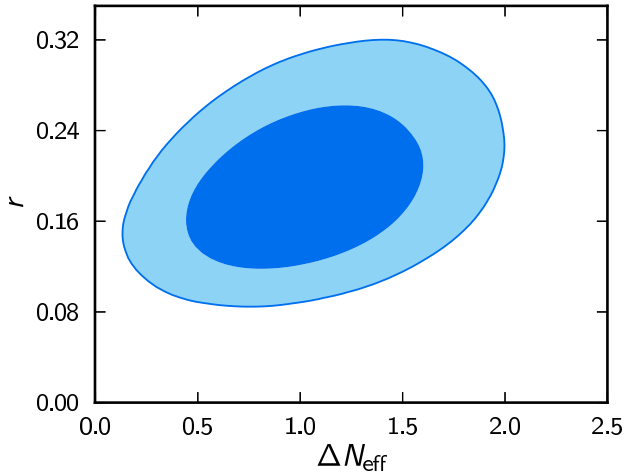


FIG. 2. Early Universe tension and neutrinos. In the  $\nu\Lambda$ CDM parameter space the EC data set favors  $\Delta N_{\text{eff}} > 0$  in order to offset the excess large angle temperature anisotropy implied by the high tensor-scalar ratio  $r$  (68%, 95% contours here and below). This in turn is driven by the degeneracy between  $\Delta N_{\text{eff}}$  and  $n_s$  illustrated in Fig. 3. In brief, gravitational waves add power at low  $\ell$ , requiring larger  $n_s$  to compensate. Larger  $n_s$  then requires larger  $\Delta N_{\text{eff}}$  to agree with the higher- $\ell$  CMB.

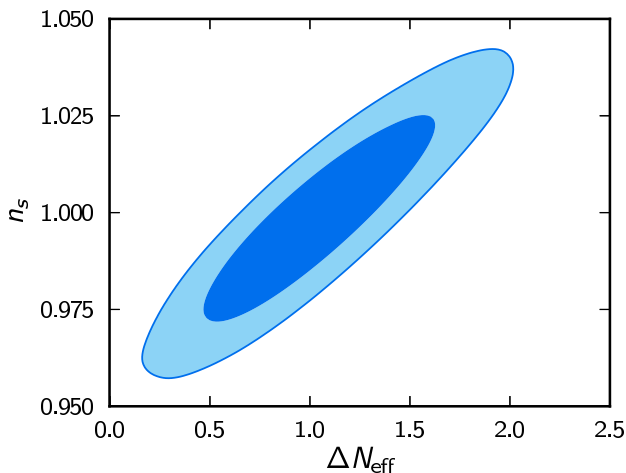


FIG. 3. In the  $\nu\Lambda$ CDM parameter space the EC data set allows a positive change in the tilt when  $\Delta N_{\text{eff}}$  is increased explaining the mechanism by which the large angle temperature anisotropy is reduced.

in the CL data set and its possible resolution in the  $\nu\Lambda$ CDM model space independently of the EC data. Fig. 6 shows the  $\Delta N_{\text{eff}} - m_s$  plane. The CL data imply  $\Delta N_{\text{eff}} = 0.62 \pm 0.28$  and  $m_s = 0.48 \pm 0.15$  eV in agreement with Ref. [14], strongly excluding the minimal neutrino model at  $\Delta N_{\text{eff}} = 0$  and  $m_s = 0$ . Without tensors the C component of the CL data set places an upper limit on  $\Delta N_{\text{eff}}$  that disfavors  $\Delta N_{\text{eff}} = 1$ . Thus the Hubble constant inferred is  $h = 0.70 \pm 0.01$ , which is consistent with measurements but on the low side. Meanwhile, the clus-

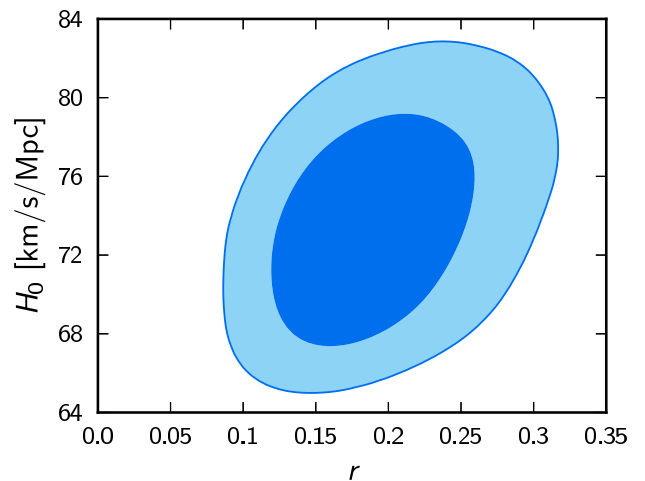
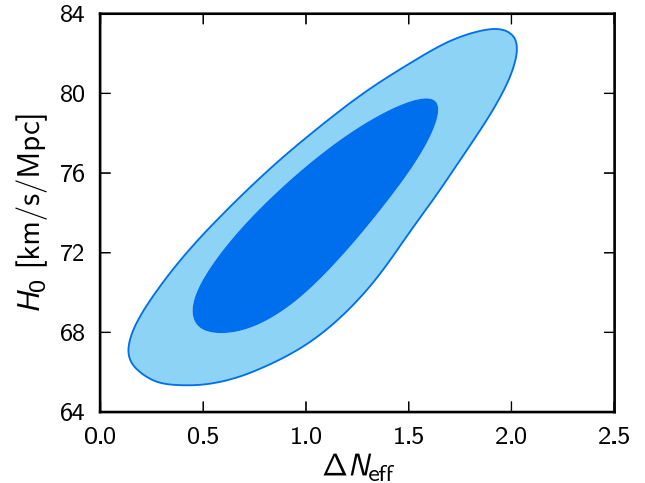


FIG. 4. By allowing for tensors and neutrinos, the EC data set in the  $\nu\Lambda$ CDM model favors higher values for  $H_0$ . Note that the actual measurements of  $H_0$  are *not* imposed here as a prior – the BICEP2 central value of  $r$  in  $\nu\Lambda$ CDM predicts an  $H_0$  in concordance with observations.

ter abundance data in the CL data set dominates the mass constraint. Note that we do not consider the impact of systematic errors on the determination of cluster masses here. In Ref. [14], it was shown that the preference for a large  $m_s$  would only be eliminated if the masses are underestimated by  $\sim 30\%$  which is large compared with the 9% uncertainty quoted in Ref. [29]. The full list of parameter constraints is given in Tab. II.

Finally we consider the combined early and late Universe (ECL) data sets in the full  $\nu\Lambda$ CDM parameter space. By including tensors in the model, we again both enable a larger  $N_{\text{eff}}$  and simultaneously fit the tensor results of BICEP2 and  $H_0$  measurements. We find that the preference for an extra massive neutrino has increased in the joint data over the CL case, especially for  $\Delta N_{\text{eff}}$ . As shown in Fig. 7 and Tab. II,  $\Delta N_{\text{eff}} = 0.98 \pm 0.26$  and  $m_s = 0.52 \pm 0.13$  eV or  $3.8\sigma$  and  $4\sigma$  evidence respectively. In particular, adding tensors closes off solutions

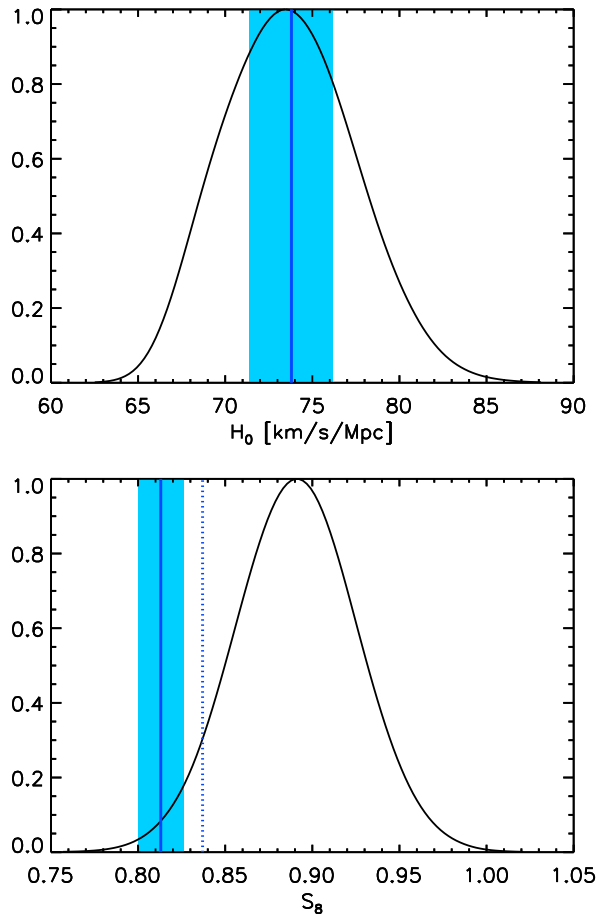


FIG. 5.  $H_0$  and  $S_8$  posterior probability distributions in the  $\nu\Lambda$ CDM parameter space using early Universe (EC) data alone compared with the late Universe measurements. To emphasize, the black 1D posteriors plotted here have been derived without any use of local Universe data. The addition of neutrinos and tensors makes the  $H_0$  posterior fully compatible with measurements (bands) and  $S_8$  substantially more compatible, though some residual tension remains. The dotted line represents the shift in the central value of the cluster abundance measurements under the assumption of a 9% systematic increase in cluster masses.

where  $H_0$  is altered by adding energy density at recombination through  $m_s$  at  $\Delta N_{\text{eff}} \rightarrow 0$  (cf. Figs. 6, 7). In addition, the distribution of the helium fraction for this combined data set is consistent with the Big Bang Nucleosynthesis measurements (see Fig. 9).

These conclusions could weaken if there were systematic problems in the cluster abundance measurements (as suggested, for example, by Ref. [30]),  $H_0$  measurements [31] or in the small-scale CMB data [32]. Ref. [33] emphasizes that the tension between CMB + BAO data and the cluster measurements is not fully resolved by neutrinos, consistent with Fig. 5, and interpret this as an indication that the cluster data is not robust. Even without the cluster data, the neutrino solution is favored in order to satisfy  $H_0$ , BAO and BICEP2 data simultaneously with the C data. In fact it is the agreement

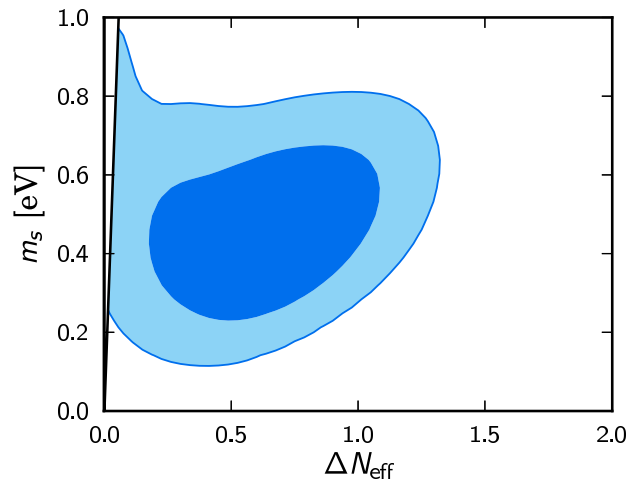


FIG. 6. Local Universe tension and neutrinos. The CL data set in the  $\nu\Lambda$ CDM parameter space strongly disfavors the minimal neutrino model with  $\Delta N_{\text{eff}}=0$  and  $m_s = 0$ . This agrees with Ref. [14–16], and comes about because local  $H_0$  measurements and local cluster abundance measurements add coherently in the direction of preferring new neutrino physics. Note that the line at  $m_s = 10(\Delta N_{\text{eff}})^{3/4}$  eV represents the prior on the physical mass.

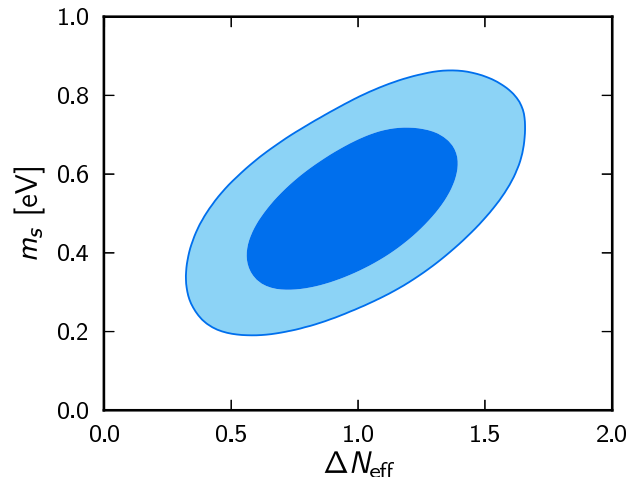


FIG. 7. Joint evidence for sterile massive neutrino in the combined ECL data set and  $\nu\Lambda$ CDM model. The minimal neutrino model of  $\Delta N_{\text{eff}} = 0$ ,  $m_s = 0$ , is rejected at even higher confidence than in the CL- $\nu\Lambda$ CDM combination and more strongly favors  $\Delta N_{\text{eff}} > 0$  (cf. Fig. 6). Note also that the same prior on  $m_s$  vs.  $\Delta N_{\text{eff}}$  has been imposed here as in Fig. 6; we do not shade the excluded region since these contours have not been distorted by this prior.

with BAO that make the single biggest contribution to the likelihood improvement from neutrinos (see Tab. III) and what is limiting the neutrino explanation is mainly a small tension with SPT/ACT. Furthermore compared with the  $\Lambda$ CDM model that best fits the C data alone, the  $\nu\Lambda$ CDM maximum likelihood model is actually a better fit to the BAO data itself and improves  $H_0$  agreement by  $2\Delta \ln L \approx 6.2$ . The net improvement in maximum like-



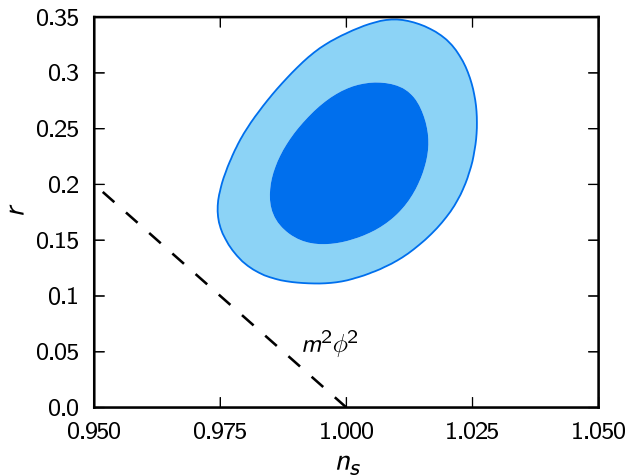


FIG. 8. Inflationary implications from the combined ECL data set and  $\nu r\Lambda\text{CDM}$  model. Inflationary models with nearly scale invariant tilt and  $r \approx 0.2$  tensor-to-scalar ratio are favored. While this region is allowed in slow roll inflation, models with featureless power law potentials such as  $m^2\phi^2$  do not have trajectories (dashed line) that intersect this region.

likelihood from adding neutrinos with the ECL data sets is  $2\Delta \ln L \approx -24$ .

	$r\Lambda\text{CDM}$ (ECL)	$\nu r\Lambda\text{CDM}$ (ECL)
Planck	18.15	7.37
WP	-0.34	-1.03
SPT/ACT	1.03	4.85
BAO	10.56	-0.36
$H_0$	-6.37	-6.20

TABLE III. Changes in the individual contributions to  $2\ln \mathcal{L}$  relative to the  $\Lambda\text{CDM}$  maximum likelihood model with "C" data.

We close with a brief mention of the inflationary consequences of our analysis. In our final analysis, we find  $n_s \sim 1$  and  $r \sim 0.2$ . Such models are allowed within the framework of slow roll inflation since they do not have a large running of the tilt. However, they fall outside the class of simple featureless monomial potentials (see Fig. 8). To achieve nearly exact scale invariance, an inflationary potential must have its slope and curvature partially cancel in their effect on the tilt, a less typical situation. There is a relative dearth of such models in the literature (see e.g. [35]), although predictions for such models can be found, for example, in Refs. [36–38].

### III. DISCUSSION

We have shown that the tension introduced by the detection of large amplitude gravitational wave power

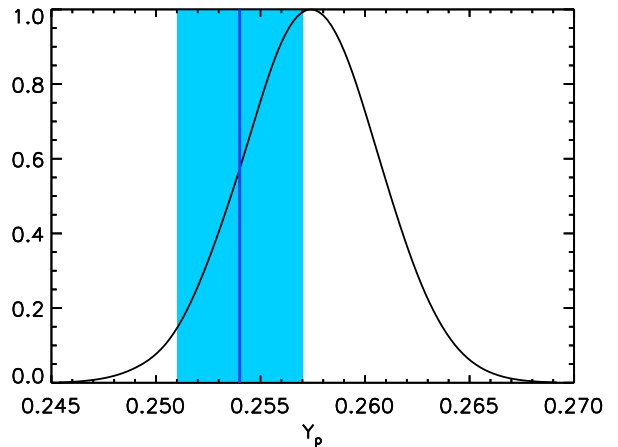


FIG. 9. Distribution of the helium fraction for the combined ECL data set and  $\nu r\Lambda\text{CDM}$  model compared with the BBN measurements (band) [34].

by the BICEP2 experiment with temperature anisotropy measurements is alleviated in a model with an extra sterile neutrino. The relativistic energy density required to alleviate this early Universe tension is the same as that required to resolve the late Universe tension of acoustic distance measures with local Hubble constant measurements. Combined they imply a  $\Delta N_{\text{eff}} = 0.98 \pm 0.26$ . Note that the ACT/SPT data already limit the upper range of allowed  $\Delta N_{\text{eff}}$ , and so this explanation of the early and late Universe tensions can be tested with more data from high multipole CMB temperature and polarization observations. Conversely, it would weaken if extra evidence for alternate inflationary or foreground explanations of the early Universe tension is found.

By making the sterile neutrino massive, the tension with growth of structure measurements can simultaneously be alleviated. The combined constraint on the effective mass is  $m_s = 0.52 \pm 0.13$  eV. This preference for high neutrino mass(es) is mainly driven by the cluster data set (cf. Ref. [39] who find upper limits without clusters). Compared with analyses that do not include gravitational waves, the sterile neutrino suggested here has a smaller expected physical mass, thanks to the generally larger values of  $\Delta N_{\text{eff}}$  that we find (recall the thermal conversion formula:  $m_s^{\text{th}} = m_s / (\Delta N_{\text{eff}})^{3/4}$ ). At the upper range of  $\Delta N_{\text{eff}}$ , it is thus somewhat less likely that this sterile neutrino could explain anomalies in short baseline and reactor neutrino experiments (see Refs. [40, 41] for reviews).

If future data or analyses lead to increased mass estimates for the clusters, that change would weaken the preference for a non-zero  $m_s$  by increasing  $S_8$ , giving better concordance with the basic  $\Lambda\text{CDM}$  prediction. However, the preference can only be eliminated if the systematic shift is roughly triple the 9% estimate; that estimate is derived from comparisons of a variety of X-ray, optical, Sunyaev-Zel'dovich, and lensing observables (see e.g. [42]

for a recent assessment).

Taken at face value, these results leave us with a potentially very different cosmological standard model. Gravitational waves are nearly indisputable evidence for an inflationary epoch, but the lack of a significant primordial tilt compared with  $r$  would suggest somewhat unusual inflationary physics is at play where the impact of the slope and curvature of the inflationary potential partially cancelled each other. On the other hand, the new neutrino physics favored here is less contrived than that proposed in Ref. [14–16]: we are now allowed  $\Delta N_{\text{eff}} = 1$ , which is in better accord with a “theory prior” that the sterile neutrino would be fully populated by oscillations with active neutrinos for typical mixing angles. Meanwhile, we see somewhat less residual tension between the early and late Universe, especially if galaxy clusters are indeed a bit more massive than we have assumed in our main analysis.

Each of these new ingredients will soon be cross checked by a wide variety of upcoming observations. If all are confirmed, observational cosmology will have provided not one but two clear discoveries of particle physics beyond the Standard Model within a short space of time,

giving long sought clear guidance for how to advance physics into the future.

## ACKNOWLEDGMENTS

During completion of this work a similar study appeared [43]; our addition of the SPT/ACT data sets place stronger upper limits on the allowed  $\Delta N_{\text{eff}}$ . Ref. [44] also finds preference for an extra relativistic species when adding BICEP2 data, but they do not include the cluster data in their analysis, which constrain the mass. We thank R. Keisler, M. LoVerde and M. Turner for useful conversations. CD was supported by the National Science Foundation grant number AST-0807444, NSF grant number PHY-088855425, and the Raymond and Beverly Sackler Funds. MW was supported by a James Arthur Postdoctoral Fellowship. DHR was supported by the KICP and the Research Computing Center at the University of Chicago. WH was supported at the KICP through grants NSF PHY- 0114422 and NSF PHY-0551142 and an endowment from the Kavli Foundation, and by U.S. Dept. of Energy contract DE-FG02- 90ER-40560.

- 
- [1] P. Ade *et al.* (BICEP2 Collaboration), (2014), arXiv:1403.3985 [astro-ph.CO].
  - [2] P. Ade *et al.* (Planck Collaboration), (2013), arXiv:1303.5076 [astro-ph.CO].
  - [3] R. Flauger, J. C. Hill, and D. N. Spergel, (2014), arXiv:1405.7351 [astro-ph.CO].
  - [4] M. J. Mortonson and U. Seljak, (2014), arXiv:1405.5857 [astro-ph.CO].
  - [5] J. B. Dent, L. M. Krauss, and H. Mathur, (2014), arXiv:1403.5166 [astro-ph.CO].
  - [6] A. Moss and L. Pogosian, (2014), arXiv:1403.6105 [astro-ph.CO].
  - [7] J. Lizarraga, J. Urrestilla, D. Daverio, M. Hindmarsh, M. Kunz, *et al.*, (2014), arXiv:1403.4924 [astro-ph.CO].
  - [8] M. J. Mortonson and W. Hu, Phys.Rev. **D81**, 067302 (2010), arXiv:1001.4803 [astro-ph.CO].
  - [9] C. Bonvin, R. Durrer, and R. Maartens, (2014), arXiv:1403.6768 [astro-ph.CO].
  - [10] C. R. Contaldi, M. Peloso, and L. Sorbo, (2014), arXiv:1403.4596 [astro-ph.CO].
  - [11] V. Miranda, W. Hu, and P. Adshead, (2014), arXiv:1403.5231 [astro-ph.CO].
  - [12] K. N. Abazajian, G. Aslanyan, R. Easther, and L. C. Price, (2014), arXiv:1403.5922 [astro-ph.CO].
  - [13] M. Kawasaki and S. Yokoyama, (2014), arXiv:1403.5823 [astro-ph.CO].
  - [14] M. Wyman, D. H. Rudd, R. A. Vanderveld, and W. Hu, Phys.Rev.Lett. **112**, 051302 (2014), arXiv:1307.7715 [astro-ph.CO].
  - [15] J. Hamann and J. Hasenkamp, JCAP **1310**, 044 (2013), arXiv:1308.3255 [astro-ph.CO].
  - [16] R. A. Battye and A. Moss, Phys.Rev.Lett. **112**, 051303 (2014), arXiv:1308.5870 [astro-ph.CO].
  - [17] Z. Hou, C. Reichardt, K. Story, B. Follin, R. Keisler, *et al.*, Astrophys.J. **782**, 74 (2014), arXiv:1212.6267 [astro-ph.CO].
  - [18] M. Gonzalez-Garcia, M. Maltoni, J. Salvado, and T. Schwetz, JHEP **1212**, 123 (2012), arXiv:1209.3023 [hep-ph].
  - [19] A. Lewis and S. Bridle, Phys. Rev. **D66**, 103511 (2002), astro-ph/0205436.
  - [20] C. Bennett, D. Larson, J. Weiland, N. Jarosik, G. Hinshaw, *et al.*, (2012), arXiv:1212.5225 [astro-ph.CO].
  - [21] S. Das, T. Louis, M. R. Nolte, G. E. Addison, E. S. Battistelli, *et al.*, (2013), arXiv:1301.1037 [astro-ph.CO].
  - [22] C. Reichardt, L. Shaw, O. Zahn, K. Aird, B. Benson, *et al.*, Astrophys.J. **755**, 70 (2012), arXiv:1111.0932 [astro-ph.CO].
  - [23] R. Keisler, C. Reichardt, K. Aird, B. Benson, L. Bleem, *et al.*, Astrophys.J. **743**, 28 (2011), arXiv:1105.3182 [astro-ph.CO].
  - [24] A. G. Riess, L. Macri, S. Casertano, H. Lampeitl, H. C. Ferguson, *et al.*, Astrophys.J. **730**, 119 (2011), arXiv:1103.2976 [astro-ph.CO].
  - [25] L. Anderson, E. Aubourg, S. Bailey, D. Bizyaev, M. Blanton, *et al.*, Mon.Not.Roy.Astron.Soc. **428**, 1036 (2013), arXiv:1203.6594 [astro-ph.CO].
  - [26] N. Padmanabhan, X. Xu, D. J. Eisenstein, R. Scalzo, A. J. Cuesta, *et al.*, Mon.Not.Roy.Astron.Soc. **427**, 2132 (2012), arXiv:1202.0090 [astro-ph.CO].
  - [27] C. Blake, E. Kazin, F. Beutler, T. Davis, D. Parkinson, *et al.*, Mon.Not.Roy.Astron.Soc. **418**, 1707 (2011), arXiv:1108.2635 [astro-ph.CO].
  - [28] F. Villaescusa-Navarro, F. Marulli, M. Viel, E. Branchini, E. Castorina, *et al.*, JCAP **1403**, 011 (2014),

- arXiv:1311.0866 [astro-ph.CO].
- [29] R. A. Burenin and A. A. Vikhlinin, *Astronomy Letters* **38**, 347 (2012), arXiv:1202.2889 [astro-ph.CO].
  - [30] E. Rozo, E. S. Rykoff, J. G. Bartlett, and A. Evrard, *mnras* **438**, 49 (2014), arXiv:1204.6301 [astro-ph.CO].
  - [31] G. Efstathiou, (2013), arXiv:1311.3461 [astro-ph.CO].
  - [32] D. Spergel, R. Flauger, and R. Hlozek, (2013), arXiv:1312.3313 [astro-ph.CO].
  - [33] B. Leistedt, H. V. Peiris, and L. Verde, *Phys.Rev.Lett.* **113**, 041301 (2014), arXiv:1404.5950 [astro-ph.CO].
  - [34] Y. Izotov, G. Stasinska, and N. Guseva, (2013), arXiv:1308.2100 [astro-ph.CO].
  - [35] J. Martin, C. Ringeval, and V. Vennin, (2013), arXiv:1303.3787 [astro-ph.CO].
  - [36] J. D. Barrow and A. R. Liddle, *Phys.Rev.* **D47**, 5219 (1993), arXiv:astro-ph/9303011 [astro-ph].
  - [37] J. D. Barrow, A. R. Liddle, and C. Pahud, *Phys.Rev.* **D74**, 127305 (2006), arXiv:astro-ph/0610807 [astro-ph].
  - [38] M. Czerny, T. Higaki, and F. Takahashi, (2014), 10.1016/j.physletb.2014.05.041, arXiv:1403.5883 [hep-ph].
  - [39] L. Verde, S. M. Feeney, D. J. Mortlock, and H. V. Peiris, (2013), arXiv:1307.2904 [astro-ph.CO].
  - [40] J. M. Conrad, W. C. Louis, and M. H. Shaevitz, *Ann.Rev.Nucl.Part.Sci.* **63**, 45 (2013), arXiv:1306.6494 [hep-ex].
  - [41] K. Abazajian, M. Acero, S. Agarwalla, A. Aguilar-Arevalo, C. Albright, *et al.*, (2012), arXiv:1204.5379 [hep-ph].
  - [42] E. Rozo, E. S. Rykoff, J. G. Bartlett, and A. E. Evrard, (2013), arXiv:1302.5086 [astro-ph.CO].
  - [43] J.-F. Zhang, Y.-H. Li, and X. Zhang, (2014), arXiv:1403.7028 [astro-ph.CO].
  - [44] E. Giusarma, E. Di Valentino, M. Lattanzi, A. Melchiorri, and O. Mena, (2014), arXiv:1403.4852 [astro-ph.CO].